BAYER PATTERN BASED CFA ZOOMING / CFA INTERPOLATION FRAMEWORK

R. Lukac[1] *K. Martin*[1] *K.N. Plataniotis*[1] *B. Smolka*[2+] *A.N. Venetsanopoulos*[1]

[1] The Edward S. Rogers Sr. Department of ECE, University of Toronto, 10 King's College Road, Toronto, Ontario M5S 3G4, Canada, *e-mails: {lukacr, kmartin, kostas, anv}@dsp.utoronto.ca*
[2] Department of Automatic Control, Silesian University of Technology, Akademicka 16 Str., 44-101 Gliwice, Poland, *e-mail: bsmolka@ia.polsl.gliwice.pl*

ABSTRACT

A unified framework for Bayer pattern based single-sensor imaging devices is introduced. Operating on the Bayer color filter array (CFA) data, the method performs CFA image zooming and full color image reconstruction in a cost-effective way making the system practical for hardware implementation. The high-level system components, namely CFA zooming, CFA interpolation and CFA based correction step utilize a color-ratio model and an edge-sensing mechanism to produce naturally colored and sharp, enlarged output. Simulation studies presented here indicate that the new method produces excellent results and outperforms other approaches in terms of both objective and subjective evaluation measures.

1. INTRODUCTION

Single-sensor digital imaging devices typically use a charge coupled device (CCD) or a complementary metal-oxide semiconductor (CMOS), combined with a color filter array (CFA) to separate incoming light into a specific spatial arrangement of color components. The Bayer pattern (*Figure 1a*) [2] is the most common CFA, providing a mosaic of Red (R), Green (G), and Blue (B) color components.

Technological advances have allowed for the miniaturization of single-sensor cameras resulting in their being embedded in a myriad of consumer electronic devices. Many of these devices, such as mobile phones and personal digital assistants (PDAs), are restricted in their optical capabilities and computational resources and thus provide limited functionality and quality of output. To provide high-quality enlarged camera output in such an imaging device, a unified CFA image processing framework is introduced here. The framework unifies three algorithmic steps (CFA zooming, CFA interpolation and CFA based correction step) designed for cost-effective hardware implementations in single-sensor cameras. The employed edge-sensing mechanism tracks varying image statistics while a color-ratio model is used in each of the algorithmic steps to avoid color artifacts in the output. Therefore, the unified framework produces the enlarged, full color camera output as a sharp, visually pleasing color image.

2. PROPOSED SOLUTION

Let us consider a $K_1 \times K_2$ Bayer CFA image $\mathbf{b} : Z^2 \rightarrow Z^3$ representing a two-dimensional matrix of three-component RGB vectors $\mathbf{b}_{(m,n)} = [b_{(m,n)1}, b_{(m,n)2}, b_{(m,n)3}]$ located in the spatial position (m,n), for $m = 1,2,...,K_1$ and $n = 1,2,...,K_2$.

+ Supported by the KBN grant 4T11F01824.

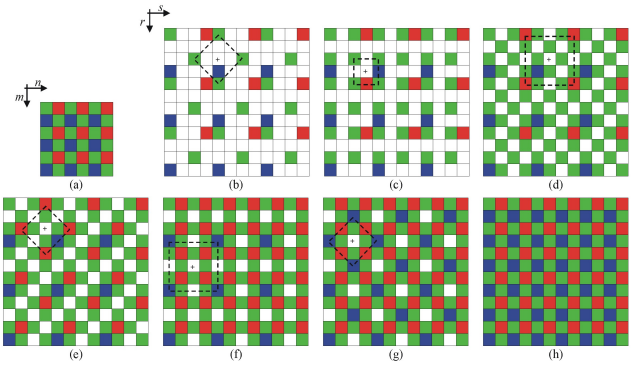

Figure 1: (a) The Bayer CFA pattern and (b-h) the spatial arrangements of the CFA components obtained applying the proposed CFA zooming steps.

Based on the Bayer CFA pattern structure (*Figure 1a*), only one color component $b_{(m,n)k}$, for $k = 1,2,3$, is available for each spatial location. Thus, $\mathbf{b}_{(m,n)} = [b_{(m,n)1}, 0, 0]$ corresponds to the R CFA component for (odd m, even n), $\mathbf{b}_{(m,n)} = [0, 0, b_{(m,n)3}]$ corresponds to the B CFA component for (even m, odd n) and $\mathbf{b}_{(m,n)} = [0, b_{(m,n)2}, 0]$ corresponds to the G CFA component for the rest of spatial positions.

The proposed camera image processing system is comprised of three distinct, yet interconnected, components: a) CFA zooming to generate a higher resolution Bayer CFA image from the original CFA data; b) CFA interpolation to generate a full color image from the higher resolution CFA image; and c) postprocessing or CFA based correction step to reduce distracting artifacts and enhance sharpness in the final output.

2.1 CFA Zooming

For simplicity, consider a zooming factor $\lambda = 2$. Since the enlarged Bayer CFA image must exactly follow the structure of the Bayer pattern, the original CFA data are assigned unique positions in a $\lambda K_1 \times \lambda K_2$ zoomed image $\mathbf{x}$. Using the approach of [7], $\mathbf{x}_{(2m-1,2n)} = \mathbf{b}_{(m,n)}$ corresponds to the R component for (odd m, even n), whereas $\mathbf{x}_{(2m,2n-1)} = \mathbf{b}_{(m,n)}$ corresponds to the B component for (even m, odd n). For the rest of locations (m,n) in the original Bayer CFA image $\mathbf{b}$, the sample $\mathbf{x}_{(2m-1,2n-1)} = \mathbf{b}_{(m,n)}$ in the enlarged CFA image $\mathbf{x}$ depicted in *Figure 1b* corresponds to the G component.

Assuming that (r,s), for $r = 1,2,...,\lambda K_1$ and $s = 1,2,...,\lambda K_2$, denotes the spatial position in the enlarged image $\mathbf{x}$, missing G components $x_{(r,s)2}$ of the enlarged Bayer

image $\mathbf{x}$ are generated using a weighted sum of the surrounding original G components $x_{(i,j)2}$ as follows:

$$x_{(r,s)2} = \sum_{(i,j)\in\zeta} w_{(i,j)} x_{(i,j)2} \tag{1}$$

where (r,s) is the location at the centre of the diamond-shaped structure of the four original G components described as $\zeta = \{(r-2,s),(r,s-2),(r,s+2),(r+2,s)\}$. The normalized weights are generated via $w_{(i,j)} = u_{(i,j)} / \sum_{(g,h)\in\zeta} u_{(g,h)}$, where the positive edge-sensing coefficients $u_{(i,j)}$ are defined as follows:

$$u_{(i,j)} = \frac{1}{1 + \sum_{(g,h)\in\zeta} |x_{(i,j)k} - x_{(g,h)k}|} \tag{2}$$

It should be mentioned that k in (2) always corresponds to k describing the interpolated component and therefore, $k = 2$ in (1). In (2), the denominator incorporates an aggregate absolute difference between the CFA input located at (i,j) and the rest of the CFA inputs described by ζ. For an outlying value $x_{(i,j)2}$ that is highly dissimilar to the rest of the values, the aggregate distance will approach infinity and $u_{(i,j)}$ will approach zero, thus decreasing the emphasis on $x_{(i,j)2}$ in generating $x_{(r,s)2}$. Alternatively, if $x_{(i,j)2}$ is similar to the other values defined by ζ, the weight $u_{(i,j)}$ will approach a maximum value of unity. This methodology preserves edge features by detecting the trend of the surrounding components.

To complete the remaining missing G components, (1) is repeated with (r,s) located at the centre of the square-shaped structure (*Figure 1c*) described via $\zeta = \{(r-1,s-1),(r-1,s+1),(r+1,s-1),(r+1,s+1)\}$. The structure incorporates two original G components and two interpolated G components from the previous step. The weights $w_{(i,j)}$ are again calculated via (2) with $k = 2$ and the square-shaped structure ζ.

To constitute the missing R (and B) components, a local color-ratio model [3],[9] is employed. For each position that requires the estimation of an R (or B) component, a local R/G (or B/G) ratio is generated using surrounding positions. Since G components are not present in the same locations as the R (or B) components, adjacent surrounding G components with the identical shift on the image lattice are used to create the color-ratios. The missing R (or B) component at the centre of the surrounding structure is estimated using the surrounding color-ratios and the G component adjacent to the centre. This takes advantage of the expected relative uniformity of the local color-ratios and the abundance of available green information, which is more accurate due to a twice as frequent occurrence of the original G CFA components compared to the R and B components.

The R components $x_{(r,s)1}$ are obtained as follows:

$$x_{(r,s)1} = x_{(r,s-1)2} \sum_{(i,j)\in\zeta} w_{(i,j)} \{x_{(i,j)1} / x_{(i,j-1)2}\} \tag{3}$$

where (r,s) is the location at the centre of the square-shaped structure shown in *Figure 1d*. The structure is formed by the original R components $x_{(i,j)1}$ positioned at locations $\zeta = \{(r-2,s-2),(r-2,s+2),(r+2,s-2),(r+2,s+2)\}$. The color-ratio $x_{(i,j)1}/x_{(i,j-1)2}$ is generated using these original

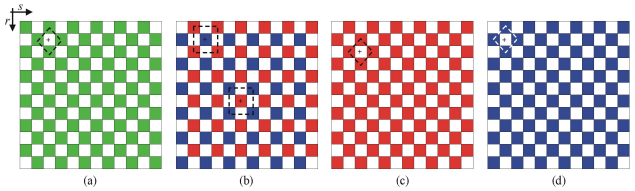

Figure 2: The spatial arrangements of the CFA components obtained applying the proposed CFA interpolation and correction steps.

R components $x_{(i,j)1}$ and the adjacent interpolated G components $x_{(i,j-1)2}$ positioned one unit to the left compared to $x_{(i,j)1}$. The missing R component $x_{(r,s)1}$ is estimated using the color-ratios and the interpolated G component $x_{(r,s-1)2}$ positioned one unit to the left. The coefficient $w_{(i,j)}$ denotes the normalized weights defined via $u_{(i,j)}$ of (2) with $k = 1$.

The remaining missing R components are generated with another repetition of (3), except with the diamond-shaped structure of both original and interpolated R components located at $\zeta = \{(r-2,s),(r,s-2),(r,s+2),(r+2,s)\}$, as shown in (*Figure 1e*).

The B components $x_{(r,s)3}$ are generated in a similar manner as follows:

$$x_{(r,s)3} = x_{(r-1,s)2} \sum_{(i,j)\in\zeta} w_{(i,j)} \{x_{(i,j)3} / x_{(i-1,j)2}\} \tag{4}$$

where $\zeta = \{(r-2,s-2),(r-2,s+2),(r+2,s-2),(r+2,s+2)\}$ denotes the positions of the original B components $x_{(i,j)3}$ in the square-shaped structure shown in *Figure 1f*. The weights are generated using (2) with $k = 3$. The G components $x_{(i-1,j)2}$, positioned one unit downward, are used in conjunction with the original B components $x_{(i,j)3}$ to generate the color-ratios. The remaining B components (*Figure 1g*) are again generated with (4), based on the diamond structure described by $\zeta = \{(r-2,s),(r,s-2),(r,s+2),(r+2,s)\}$. Performing this step the procedure produces the enlarged Bayer CFA image depicted in *Figure 1h*.

2.2 CFA Interpolation

The proposed method continues by interpolating the enlarged Bayer pattern image into a full color image. This step is unified with the previous CFA zooming step in that the same weighting and color-ratio model is utilized to estimate the missing R and B color components.

The missing G components $x_{(r,s)2}$ are estimated using (1) with the diamond-shaped structure $\zeta = \{(r-1,s),(r,s-1),(r,s+1),(r+1,s)\}$ shown in *Figure 2a*, and the weights $w_{(i,j)}$ obtained via (2) with $k = 2$. The R ($k = 1$) and B ($k = 3$) components $x_{(r,s)k}$ are then given by

$$x_{(r,s)k} = x_{(r,s)2} \sum_{(i,j)\in\zeta} w_{(i,j)} \{x_{(i,j)k} / x_{(i,j)2}\} \tag{5}$$

where $w_{(i,j)}$ are the weights (2) obtained for $k = 1$ corresponding to R components or $k = 3$ denoting B components. The interpolator of (5) is identical to (3) and (4) except that the color-ratios are generated using G components $x_{(i,j)2}$ in the same spatial position as the R or B components $x_{(i,j)k}$. The components $x_{(i,j)k}$ are now located (*Figure 2b*) at the

Figure 3: The test color images: (a) Mountains, (b) Mask, (c) Lighthouse.

centre of the square-shaped structure $\zeta = \{(r-1,s-1),(r-1,s+1),(r+1,s-1),(r+1,s+1)\}$ formed by the CFA components $x_{(i,j)k}$ with the same k as the interpolated component $x_{(r,s)k}$. The normalizing G component $x_{(r,s)2}$ used in (5) is located in the center of ζ.

The remaining missing R and B components are generated using (5) with the diamond-shaped structure $\zeta = \{(r-1,s),(r,s-1),(r,s+1),(r+1,s)\}$ shown in *Figure 2c,d*. Once this is completed, a full color image is obtained with each spatial location containing three color components.

2.3 CFA Based Correction Step

The final step in the proposed architecture is employed to reduce false color artifacts and enhance sharpness. It takes advantage of the underlying Bayer pattern present before the CFA interpolation and can be viewed as an iterative update of the components that were estimated during CFA interpolation.

First, the G components estimated during CFA interpolation are updated using a color-ratio as follows:

$$x_{(r,s)2} = x_{(r,s)k} \sum_{(i,j)\in\zeta} w_{(i,j)} \{x_{(i,j)2}/x_{(i,j)k}\} \qquad (6)$$

where $x_{(i,j)k}$ denotes the R components $k=1$ if the position (r,s) corresponds a Bayer pattern R component. Otherwise the position corresponds to a Bayer pattern B component and $k=3$. As it is shown in *Figure 2a*, the color-ratio $x_{(i,j)2}/x_{(i,j)k}$ is generated with the surrounding spatial locations $\zeta = \{(r-1,s),(r,s-1),(r,s+1),(r+1,s)\}$ containing G components $x_{(i,j)2}$ and restored R ($k=1$) or B ($k=3$) components $x_{(i,j)k}$. The edge-sensing weights $w_{(i,j)}$ used in (6) are calculated using (2) with $k=2$.

The R and B components estimated during CFA interpolation are updated in two consecutive steps. First, (5) is used to update R components on Bayer pattern B locations and B components on Bayer pattern R locations, as shown in *Figure 2b*. The square-shape mask $\zeta = \{(r-1,s-1),(r-1,s+1),(r+1,s-1),(r+1,s+1)\}$ is used to take advantage of the surrounding Bayer pattern R or B components respectively, along with the previously updated G components in the same positions. Then (5) is repeated in the remaining locations (*Figure 2c,d*) with estimated R or B components using $\zeta = \{(r-1,s),(r,s-1),(r,s+1),(r+1,s)\}$. For both steps, $w_{(i,j)}$ is calculated using (2) with either $k=1$ (updating R) or $k=3$ (updating B). This completes the correction process of all color components obtained during CFA interpolation.

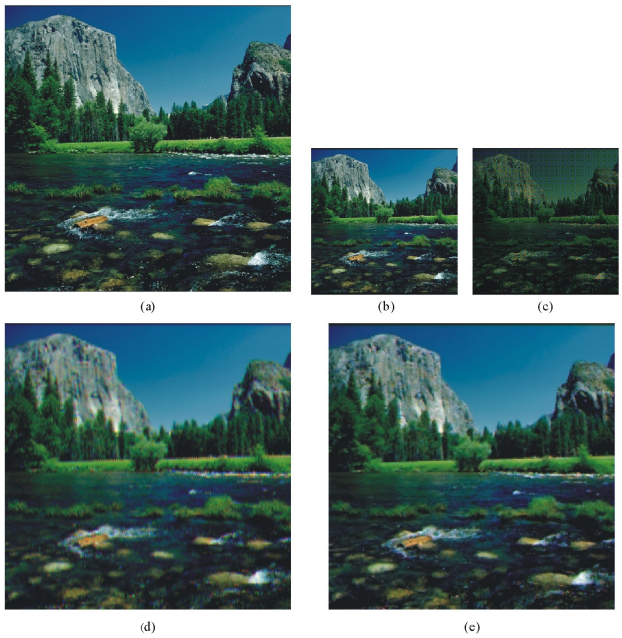

Figure 4: Processing steps performed for comparison purposes: (a) a $\lambda K_1 \times \lambda K_2$ original image $\mathbf{o}$, (b) a $K_1 \times K_2$ downsampled image $\mathbf{o_b}$, (c) a $K_1 \times K_2$ Bayer image $\mathbf{b}$ used as the started point for the methods, (d) a $\lambda K_1 \times \lambda K_2$ color image obtained by CIZ scheme, (e) a $\lambda K_1 \times \lambda K_2$ color image obtained by the proposed method.

3. EXPERIMENTAL RESULTS

A number of color images have been used to evaluate the proposed digital zooming framework. Examples are shown in *Figure 3*. Note that in order to facilitate comparisons, all images have been normalized to the standard 8-bit per channel RGB representation. Since an original Bayer image is unavailable, the evaluation approach follows the steps shown in *Figure 4*. A $\lambda K_1 \times \lambda K_2$ original color image $\mathbf{o}$ is downsampled to a $K_1 \times K_2$ color image $\mathbf{o_b}$. This image is sampled with the Bayer CFA pattern in order to obtain a test Bayer image $\mathbf{b}$ used as a starting point for testing purposes [6],[9]. The proposed unified zooming framework is evaluated by applying it to $\mathbf{b}$. The enlarged camera output $\mathbf{x}$ with size $\lambda K_1 \times \lambda K_2$ obtained using the proposed scheme is compared to the zoomed images achieved by a conventional color image zooming (CIZ) approach (bilinear CFA interpolation [6],[10] followed by bilinear image zooming [4] in the RGB color domain), as well as local CFA zooming (LZ) scheme (replication based local CFA zooming approach [1] followed by bilinear CFA interpolation).

The performance of the methods is measured via the mean absolute error (MAE), the mean square error (MSE) and the normalized color difference criterion (NCD) [8].

The objective results are summarized in Tables 1–3 and visual results are shown in Figure 5. The objective results show that the proposed scheme outperforms both the CIZ and LZ approach for all the test images using all three performance measures. The difference is most dramatic for the Mask test image due to the complex nature of the image. The proposed method produces superior results since it is able to adapt to the image structures via the edge sensing weights.

Table 1: Results obtained using the test image Mountains.

Method	*MAE*	*MSE*	*NCD*
CIZ approach	10.939	317.0	0.1701
LZ approach	11.688	362.7	0.1849
Proposed method	10.276	264.2	0.1681

Table 2: Results obtained using the test image Mask.

Method	*MAE*	*MSE*	*NCD*
CIZ approach	16.344	623.5	0.1669
LZ approach	17.736	737.2	0.1879
Proposed method	14.050	463.9	0.1449

Table 3: Results obtained using the test image Lighthouse.

Method	*MAE*	*MSE*	*NCD*
CIZ approach	9.516	318.7	0.0762
LZ approach	10.143	362.9	0.0850
Proposed method	9.008	284.8	0.0578

Figure 5: Enlarged part of the results achieved using the test image Mountains (left column), Mask (middle column) and Lighthouse (right column) and the following method: (a) original image, (b) CIZ scheme, (c) LZ scheme, (d) proposed method.

The visual results shown in Figure 5 focus on image regions containing high contrast edges which typically exhibit color artifacts upon the application of CFA zooming and interpolation schemes. As can be seen, in all cases the CIZ and LZ schemes produce color artifacts and blurriness. The proposed scheme produces little to no color artifacts while maintaining details and sharpness.

4. CONCLUSION

A new Bayer pattern based interpolation framework unifying CFA zooming, CFA interpolation and CFA based correction step has been introduced. The framework utilizes a new edge-sensing mechanism and a color-ratio model in each of its high-level components. A small number of low-complexity operations that are reused with different parameters throughout the system makes the framework attractive for hardware implementation in compact, low-cost single-sensor imaging devices in which optical zooming functionality is impractical.

By using a consistent framework which performs zooming operations before CFA interpolation, high-quality output is achieved without amplification of distracting artifacts. Applying the proposed method to the Bayer CFA data, the method produces enlarged color images pleasing for viewing. At the same time it yields excellent results in terms of commonly used objective and subjective image quality criteria and outperforms other schemes.

REFERENCES

[1] S. Battiato, G. Gallo, and F. Stanco, "A locally adaptive zooming algorithm for digital images," Image and Vision Computing, vol. 20, no. 11, pp. 805–812, Sep. 2002.

[2] B. E. Bayer, "Color imaging array," *U.S. Patent* 3 971 065, 1976.

[3] D. R. Cok, "Signal processing method and apparatus for producing interpolated chrominance values in a sampled color image signal," *US Patent* 4 642 678, 1987.

[4] H.S. Hou and H.C. Andrews, "Cubic splines for image intepolation and digital filtering," *IEEE Trans. Acoustics, Speech and Signal Proc.*, vol. 26, pp. 508-517, 1978.

[5] B. S. Hur and M. G. Kang, "High definition color interpolation scheme for progressive scan CCD image sensor," *IEEE Trans. Consumer Electronics*, vol. 47, pp. 179–186, Feb. 2001.

[6] P. Longere, Z. Xuemei, P. B. Delahunt, and D.H. Brainard, "Perceptual assessment of demosaicing algorithm performance," *Proceedings of the IEEE*, vol. 90, pp. 123–132, Jan. 2002.

[7] R. Lukac and K. N. Plataniotis, "Digital camera zooming on the colour filter array," *IEE Electronics Letters*, vol. 39, pp. 1806-1807, December 2003.

[8] K. N. Plataniotis and A. N. Venetsanopoulos, *Color Image Processing and Applications*, Springer-Verlag, 2000.

[9] R. Ramanath, W. E. Snyder, G. L. Bilbro, and W. A. Sander III, "Demosaicking methods for Bayer color arrays," *Journal of Electronic Imaging*, vol. 11, pp. 306–315, July 2002.

[10] T. Sakamoto, C. Nakanishi, and T. Hase, "Software pixel interpolation for digital still cameras suitable for a 32-bit MCU," *IEEE Transactions on Consumer Electronics*, vol. 44, pp. 1342–1352, Nov. 1998.